Chapter 2

The luminescent characteristics of Si nanocrystals and defects in SiO_2:Si^+

2.1 Abstract

The pumping-intensity dependency of nanocrystallite Silicon (nc-Si) related microphotoluminescence (μ-PL) from multirecipe Si-implanted quartz is characterized. After annealing at 1100°C for three hours, the μ-PL at 724 nm contributed by nc-Si with a diameter of about 4 nm is maximized. By increasing the pumping intensity from 10 kW/cm^2 to 300 kW/cm^2, the μ-PLs of 1-hr and 3-hr annealed Si-implanted quartz samples are red-shifted by <1.2 nm and 11 nm, respectively. The μ-PL of 3hr-annealed sample further red-shifts by 2.5 nm after pumping at 300 kW/cm^2 for one hour. Such a red-shift in PL is attributed to the anomalous quantum stark effect under strong illumination, which photo-ionizes the buried nc-Si and initiates an electric field beneath the surface of Si-implanted quartz. The measurement of accumulating charges and voltage drop during illumination primarily elucidate the correlation between red-shift in PL and the photo-ionized nc-Si induced surface electric-field.

2.2 Introduction

Si ion implantation has recently emerged as an alternative method of synthesizing Si nanocrystals (nc-Si) in SiO_2 matrix. Various photoluminescence (PL) bands from Si-implanted SiO_2 materials (SiO_2:Si^+) have been identified to originate from principle defects such as the neutral oxygen vacancy (NOV, denoted as $O_3{\equiv}Si{-}Si{\equiv}O_3$) with PL at 410-460 nm [1], and the precursor of nc-Si (E'_δ, denoted as $Si^{\uparrow}Si{-}Si$) with PL at 520-550 nm [2], among others. The high-temperature annealing of SiO_2:Si^+ usually quenches defects and formats nc-Si, providing a more pronounced near-infrared PL (700-900 nm). The nc-Si related PL wavelength depends strongly on the size of nc-Si. The Si-rich SiO_2:Si^+ material with self-assembled Si quantum dots (QDs) has attracted considerable interest for their potential use in fabricating novel light-emitting or charge-storage devices. Recently, the electric-field-dependency of the luminescence of QD-embedded materials under changing charge distribution beneath or inside the QDs has been reported and attributed to the quantum-confined Stark effect of the QDs [3,4]. The sign of the Stark shift was found to depend strongly on the change in external electric field and the built-in dipole momentum of the QD [5,6]. Sheng *et al* [7]. observed an anomalous Stark shift of the stacked InAs/GaAs self-assembled QD structure, in which a three-dimensional field drastically modified the hole state. The micro-PL (μ-PL) of QDs further indicates some extraordinary phenomena, such as the intermittent fluorescence and a long coherent time, among others

[8,9]. Unlike the size-dependent PL red-shift of nc-Si,[10,11] the correlation between pumping intensity and wavelength shift in PL of SiO_2:Si^+ materials has yet not been satisfactorily explained. This work investigates the pumping-intensity dependent μ-PL of the Si-implanted quartz prepared by multi-recipe implantation. Long-term annealed Si-implanted quartz exhibits buried nc-Si, which corresponds a red-shift in μ-PL as the pumping intensity is increased. The shifts in wavelength at various pumping intensities and durations are evaluated. The accumulating rate of surface charges and the corresponding change in the space charge field strength of the Si-implanted quartz under illumination are measured, which corroborates the effect of the electric field induced by accumulation of surface charges is more pronounced than other mechanisms.

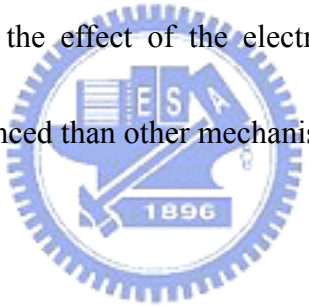

2.3 Experiment

A 1-mm-thick quartz substrate was pre-annealed for 1 hr and concurrently implanted with Si ions at 5×10^{15} ions/cm^2 at 40 keV, 1×10^{16} ions/cm^2 at 80 keV, and 2.5×10^{16} ions/cm^2 at 150 keV. The secondary-ion mass spectroscopy (SIMS) of Si-implanted quartz reveals that the Si atoms with a maximum excess density of 0.8 % are uniformly distributed at depths between 40 nm and 300 nm below the surface, this result agrees quite well with that obtained using TRIM simulation (see the Fig. 2-1). The Si-implanted quartz samples were subsequently annealed at 1100^{o}C in quartz furnace with flowing N_2 gas for 1-3 hrs.

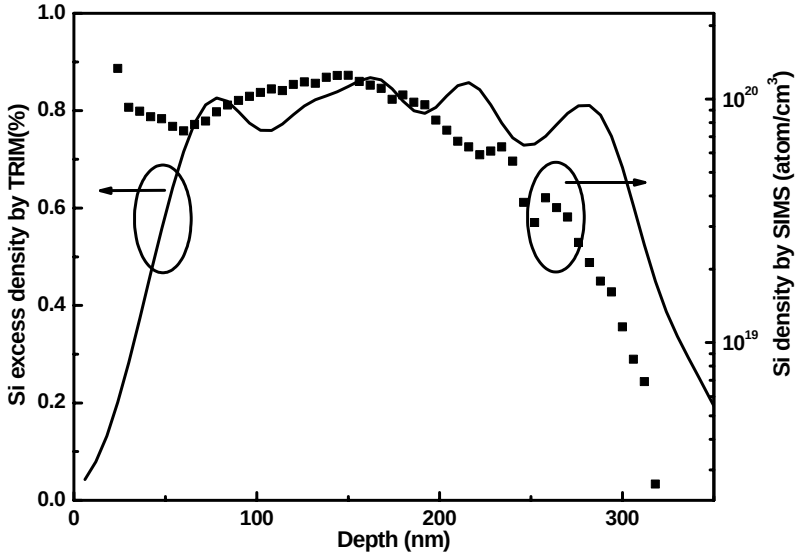

Fig. 2-1 The profile of TRIM simulation and the secondary ion mass spectrometry (SIMS).

Afterwards, a continuous-wave μ-PL measurement was performed using a 325-nm He-Cd laser with a focused spot size of 2.5 μm. The pumping intensity changes from 10 to 300 kW/cm^2. The μ-PL was detected using a fluorescence spectrophotometer (Jobin Yvon, TRIAX-320 with wavelength resolution of 0.06 nm) and a photomultiplier (Jobin Yvon, Model 1424M). A high-resistance electrometer (Keithley, 6517A) and a probe-station (Karr Suss, Munchen-Garching) were employed to measure the charges accumulated on the surface of Si-implanted quartz, with the spacing between micro-probes fixed at 100 μm.

2.4 Results and Discussion

2.4.1 The measurement of the μ-PL

Three μ-PL peaks from the pure quartz sample were observed at 410 nm, 520 nm, and

754 nm (inset of Fig. 2-2), which correspond respectively to weak oxygen-bond defects with PL at 410 nm [12], self-trapped exciton centers (irradiation-induced transient oxygen Frenkel pairs composed of an oxygen vacancy and a peroxy linkage) with PL at 515-560 nm [13,14], and Al-hole centers with PL at 729-755 nm [15].

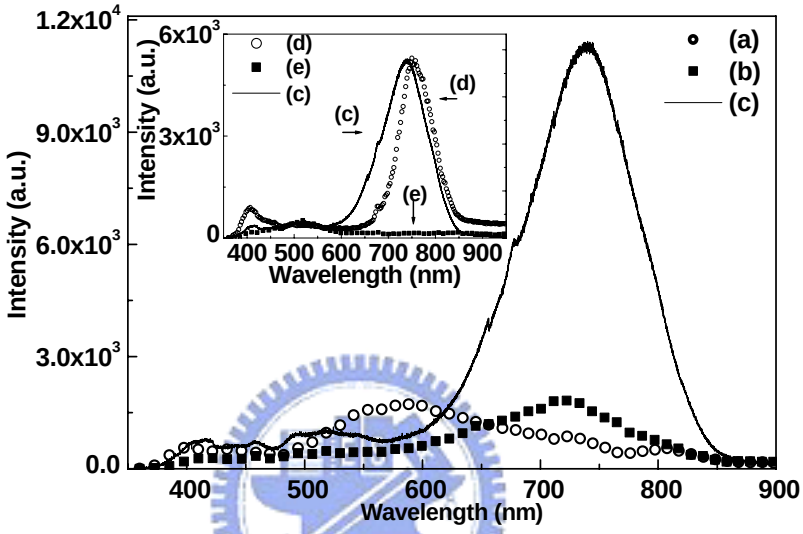

Fig. 2-2 The μ-PL spectra of Si-implanted quartz samples at (a) as-implanted condition, or annealed at 1100°C for (b) 1 hr and (c) 3 hrs. The inset figure shows the pure quartz samples (d) before and (e) after annealing at 1100 °C for 1 hr.

The Al-hole centers greatly strengthen the μ-PL since the density of residual Al in quartz is as high as 14 ppm (shows in Tab.2-1).

Table 2-1 the quartz of typical trace element composition (ppm by weight)

Na	Li	Ca	K	Al	OH
0.7 ppm	0.6 ppm	0.4 ppm	0.6 ppm	14 ppm	5 ppm

These defect-related peaks can be completely eliminated after annealing for one hour or longer, which excludes the existence of nc-Si (contribute to PL at 700-800 nm) in quartz. In

contrast, the μ-PL (in Fig. 2-2) of Si-implanted quartz includes a new peak at 550-600 nm and a weak one at 720-725 nm (shorter than that contributed by the Al-hole centers). The former PL peak attributed to the E'_{δ} defect in SiO_2 matrix diminishes during 1-hr annealing, whereas the intensity of the μ-PL at 720-725 nm is enhanced. The electron paramagnetic resonance (EPR) signal proves the presence of E'_{δ} centers in Si-implanted quartz sample. Fig. 2-3 shows the EPR spectra for the Si-implanted quartz samples before and after annealing for 1-hr.

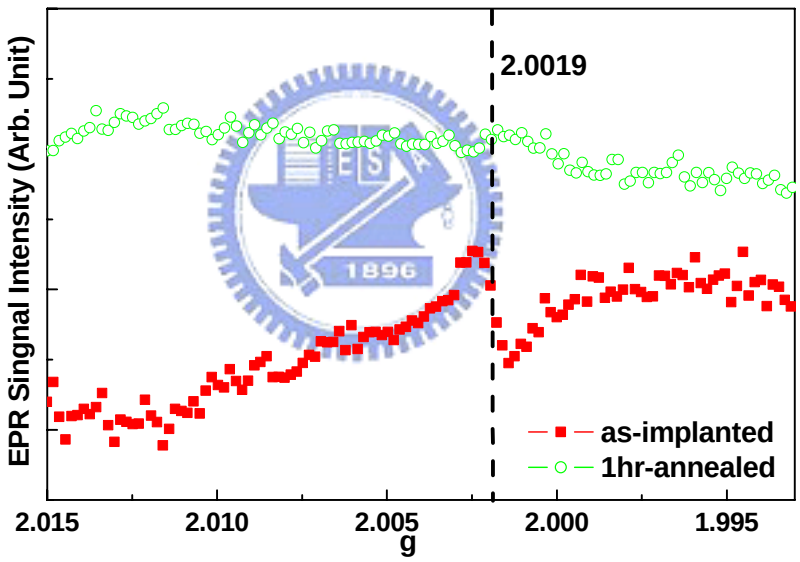

Fig. 2-3 The electron paramagnetic resonance (EPR) spectra of the as-implanted and 1-hr annealed Si-implanted quartz.

As the annealing time lengthens, most of the E'_{δ} defects are transformed into larger nc-Si in Si-implanted quartz. The correlation between the PL wavelength and the nc-Si size has been theoretically calculated and confirmed by TEM analysis. For example, Delerue *et al.*

[16] determined that the nc-Si size-dependent PL wavelength is $\lambda \cong 1.24 / (E_0 + 3.73/d^{1.39})$, where E_0 is the bandgap energy of the bulk silicon and d is the diameter of nc-Si buried in Si-implanted quartz. Mutti *et al*. [17] observed that the Si-rich SiO_2 annealed at 1000-1250^oC can efficiently precipitate nc-Si with a diameter of about 3-4 nm in the SiO_2 matrix. In our case, the enhancement of μ-PL at 724 nm from Si-implanted quartz is contributed by the buried nc-Si with a diameter of about 4 nm.

2.4.2 The temperature effect

The μ-PL wavelength of Si-implanted quartz annealed for three hours is red-shifted from 724 nm to 735 nm as the pumping intensity increases from 10 kW/cm^2 to 300 kW/cm^2 (see Fig. 2-4). In contrast, the red-shift of the μ-PL of the Si-implanted quartz annealed for one hour is only 1.2 nm, as shown in Fig. 2-5. This phenomenon cannot be attributed to the band-filling effect of excited states in nc-Si since the band-filling only causes a blue-shift. Furthermore, the required temperature change of nc-Si for such a red-shift is calculated as >100K according to $\Delta E(T) = \alpha T^2/(T+\beta)$, [18] where $\Delta E(T)$ is the change in bandgap energy as a function of substrate temperature (T), and α and β are 7.021×10^{-4} and 1108, respectively, for Si. The experimental data of n_o and k_o at different wavelengths for SiO_2 (type α, crystalline) as show in Fig. 2-6 (a), and the (b) plots the n_e and k_e of SiO_2 (type β, crystalline), which exhibit almost same results with those for n_o and k_o. In Fig.

2-7, the experiment results for wavelength-dependent transmission and absorption of the Si-implanted quartz sample are illustrated.

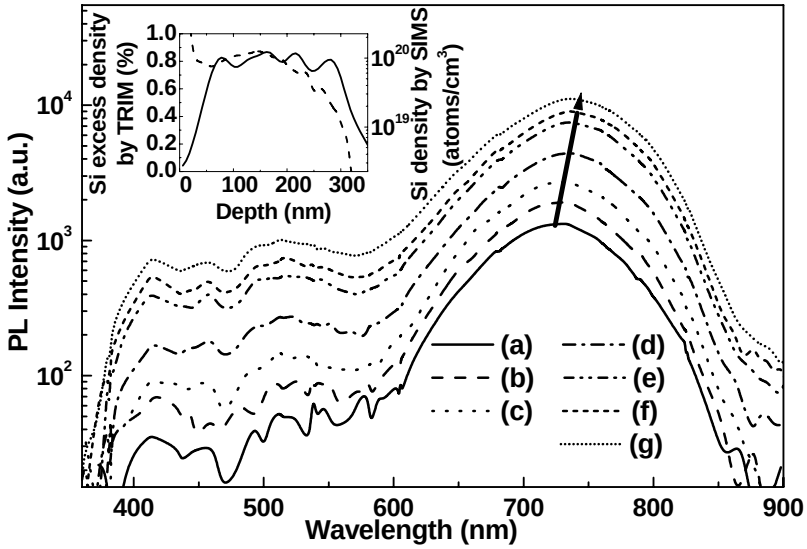

Fig. 2-4 The power dependent μ-PL spectra of the 3-hr annealed Si-implanted quartz at pumping intensity of (a) 10 kW/cm^2, (b) 25 kW/cm^2, (c) 50 kW/cm^2, (d) 100 kW/cm^2, (e) 200 kW/cm^2, (f) 250 kW/cm^2, and (g) 300 kW/cm^2. The inset figure plots the TRIM-simulated and SIMS-measured Si excess density as a function of depth.

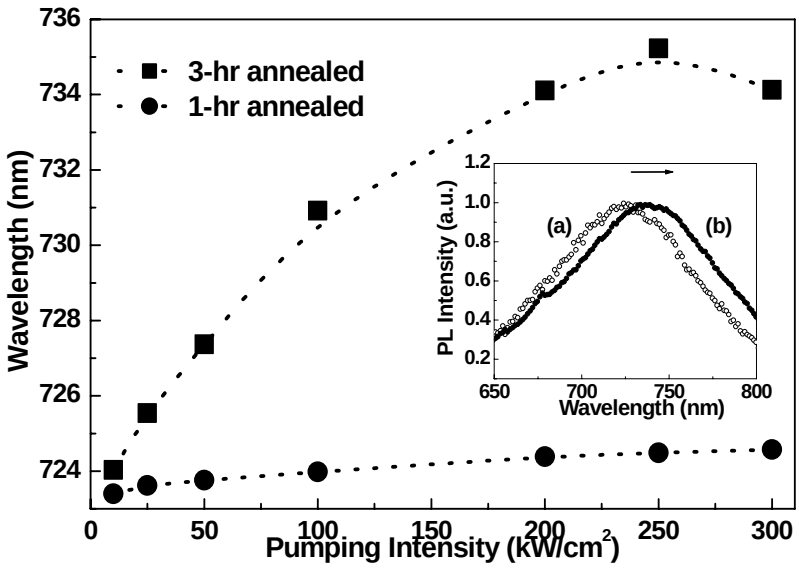

Fig. 2-5 The wavelength shift of μ-PL for 1-hr and 3-hr annealed Si-implanted quartz samples at different pumping intensity. The inset figure shows the red-shifted μ-PL spectra for the 3-hr annealed sample at pumping intensities of (a) 10 kW/cm^2 and (b) 300 kW/cm^2.

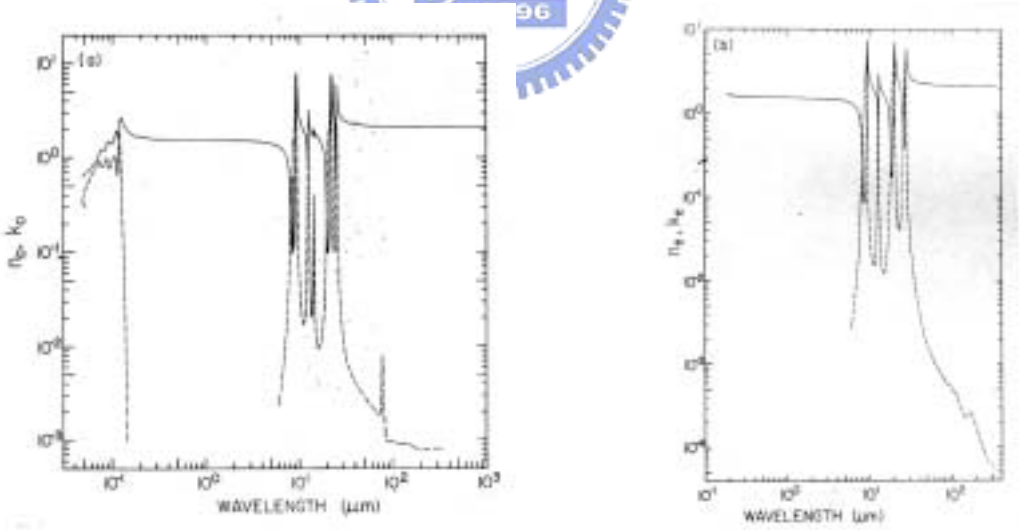

(a) (b)

Fig. 2-6 (a) n_o and k_o versus wavelength in micrometers for silicon dioxide (type α, crystalline); (b) plot of n_e and k_e versus wavelength in micrometers for silicon dioxide (type β, crystalline).

It is seen that the measured absorption coefficient is extremely small at wavelength 325 nm, and the related penetrating length (L_e >> 100 cm) is much longer than the thickness of quartz sample (thickness ~ 1 mm). Such a low absorption coefficient is unable to produce a significant substrate heating effect, which can only lead to a negligible increase in temperature of the Si-implanted quartz.

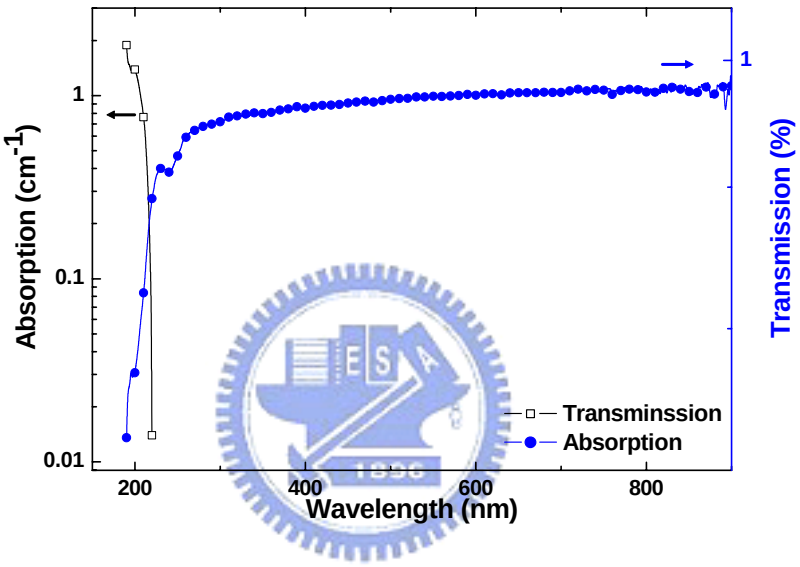

Fig. 2-7 The wavelength depended transmission and absorption curve.

A temperature controller (Newport, Model 325 with temperature resolution of 0.001°C) and a thermistor (Takanawa, 103TE-087-1P) are employed to measure the change in temperature of the Si-implanted quartz sample during the PL measurement. The thermistor with geometric size of 1 mm^2 is located beneath the illuminating point (with spacing of <100 μm). The setup is shown in Fig. 8.

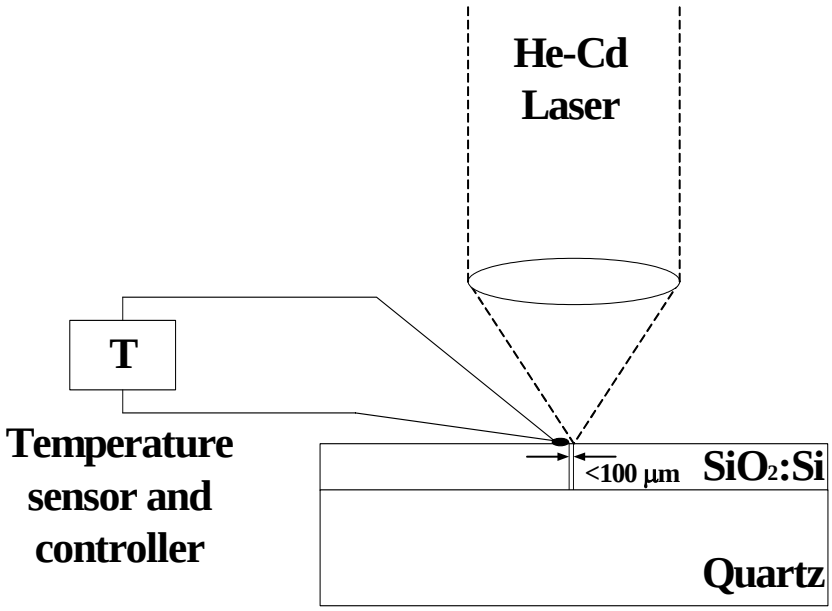

Fig. 2-8 The temperature measured setup.

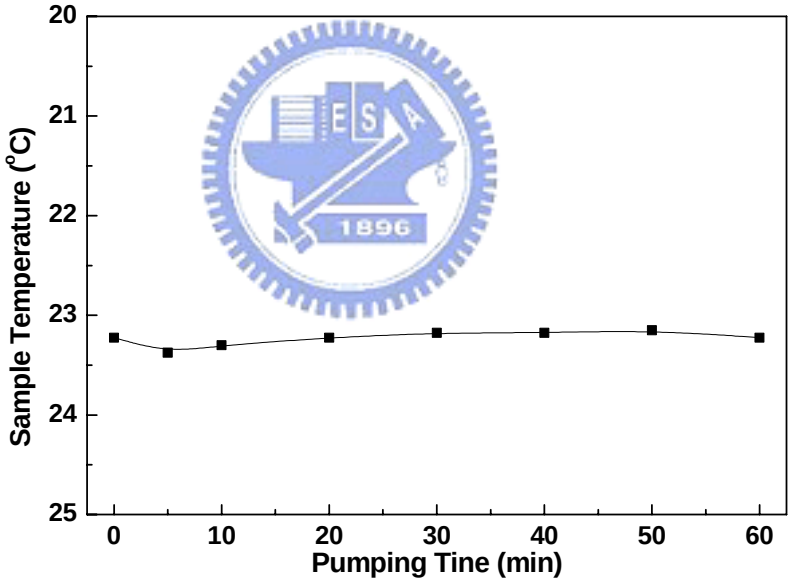

Fig. 2-9 The time dependent temperature measured.

The tiny absorption coefficient also corroborates that the substrate heating effect should not be pronounced. Following the equation of $E(T)=E_{T=0}-\alpha T^2/(T+\beta)$, [18] the maximum red shift of $\Delta\lambda=0.016$ nm can thus be evaluated from $\Delta E/\Delta T=-T(\alpha T+2\beta)/(T+\beta)^2$ under a temperature change of 0.3 ^oC, providing a negligible

heating effect on the PL response (see the Fig. 2-9). That is, the pumping induced thermal effect on the Si-implanted quartz is excluded as a cause of the red shift in PL wavelength.

2.4.3 The coupled quantum well effect

Previously, Ma *et al.* [19] have observed similar red-shift of the PL phenomenon in InAs/AlAs quantum well structure that consists of coupled QDs. As the pumping intensity is increased, the carriers captured in the coupled QDs preferentially tunnel from smaller QD to lager QD with lower energy state. [20] Two significant and neighboring PL peaks were observed as a further evidence of the occurrence of such a coupled-QD-induced PL red-shift. The carrier redistribution occurs especially when carriers are in excited states of the coupled QDs because of ground-state filling effect, which eventually results in a red-shifted and narrower PL peak. However, the Si-implanted quartz exhibits no adjacent μ-PL peaks, and coupled Si QDs can barely generated at such a low excess density of Si.

2.4.4 The quantum stark effect

Thus, the dominant mechanism of red-shifted μ-PL in Si-implanted quartz with buried nc-Si is considered to involve the first-order quantum Stark effect induced by external electric-field [21-24]. However, no external field was applied to the Si-implanted quartz instead of a strong illumination during μ-PL analysis. Hence the only possible mechanism which initiates the quantum Stark effect is attributed to the capture of carriers in nc-Si, generating an internal electric field during high-intensity pumping. This results in the

accumulation of charges beneath the surface of long-term annealed Si-implanted quartz during strong illumination. As an evidence, the measurement of accumulated surface charges on Si-implanted quartz before and after illumination is illustrated in Fig. 2-10.

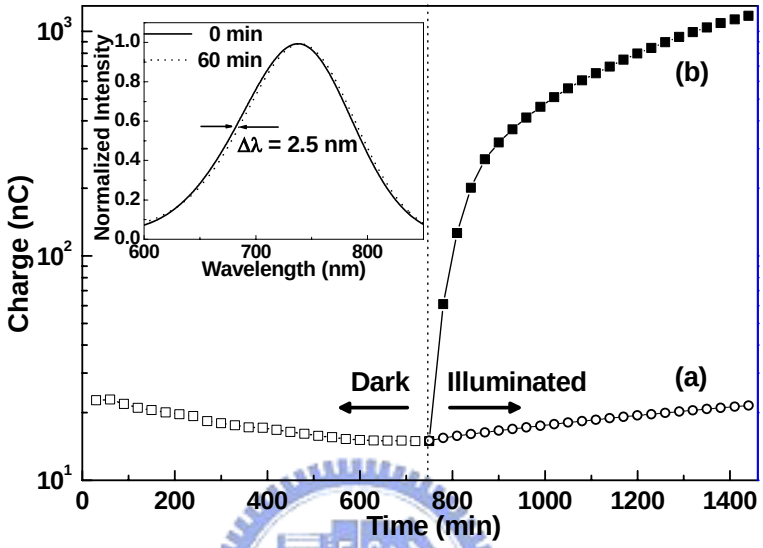

Fig. 2-10 The accumulated surface charges of (a) 1-hr annealed and (b) 3-hr annealed samples measured before and after illuminating for 12 hours. The inset figure illustrates the red-shifted μ-PL from 3-hr annealed Si-implanted quartz illuminated at 300 kW/cm^2 for 1 hour.

A decline in the residual charges is observed on the surface of Si-implanted quartz without illumination. Illumination at 300kW/cm^2 increases the surface charge from 5 nC to 1 μC within 12 hours, corresponding to a surface electric field of up to 2.47×10^4 V/cm, which is due to the extremely low density of nc-Si. In comparison, the surface charges accumulated on the 1-hr annealed sample is only 2×10^{-8} Coulomb after illumination for 12 hrs, which is due to a lower density of nc-Si precipitated in the Si-implanted quartz during 1-hr annealing. Since the nc-Si/quartz interface states recombine the photo-excited electrons

from the nc-Si, the remaining holes positively charge the nc-Si, which simultaneously build up an internal electric field from the nc-Si layer to the quartz surface. Elliman *et al*. [25] claimed that the charging effect could occur only in the oxide beneath the nc-Si/quartz interface with highest electron-hole recombination rate. As the pumping intensity is increased, the concentration of photo-excited holes captured in nc-Si and the surface electric field strength become higher, inevitably leading to the red-shift of μ-PL from Si-implanted quartz. Longer annealing duration increases the concentration and diameter of nc-Si precipitated in quartz, enlarging the red-shift of μ-PL (Fig. 2-4). Moreover, the μ-PL wavelength can also be red-shifted by extending the illumination duration at same pumping intensity. The inset in Fig. 2-10 indicates a μ-PL wavelength shift of 2.5 nm after illuminating at 300 kW/cm^2 for one hour. Note that the red-shift does not occur under low-intensity condition. These results primarily explain the build-up of internal electric field due to the accumulation of surface and captured charges in Si-implanted quartz with buried nc-Si. The Stark effect induced by strong photo-excitation in thermally annealed, Si-implanted quartz that contains nc-Si is thus elucidated.

2.5 Conclusion

In conclusion, the pumping-intensity-dependent μ-PL from multi-recipe Si-implanted quartz with 0.8 % excess Si density has been characterized. After annealing for one hour,

the weak oxygen-bond and E'_{δ} defects at 410 nm and 550 nm are eliminated, while the nc-Si with a diameter of 4 nm contributes to a strong μ-PL at central wavelength of 724 nm. The nc-Si-related μ-PL reaches a maximum after annealing at 1100°C for three hours. As the pumping density is increased from 10 kW/cm^2 to 300 kW/cm^2, the μ-PL of the irradiative defects are associated with blue-shift phenomena governed by band-filling effect. In contrast, the μ-PL wavelength of Si-implanted quartz annealed for three hours is significantly red-shift from 724 nm to 735 nm. This phenomenon cannot be well explained by either the substrate heating or the quantum-well coupling reported previously. The dominant mechanism is the anomalous quantum Stark effect induced by the built-in electric field from the buried nc-Si to the surface of Si-implanted quartz under high-intensity or long-term optical pumping. Such a red-shift in μ-PL is strongly correlated with the positively charged nc-Si, which has been corroborated by the observations of gradually accumulated charges and enlarged electric field on the surface of Si-implanted quartz during high-power illumination.

References

[1] H. S. Bae, T. G. Kim, C. N. Whang, S. Im, J. S. Yun, and J. H. Song, J. Appl. Phys. **91**, 4078 (2002).

[2] H. Nishikawa, R. Nakamura, and J. H. Stathis, Phys. Rev. B **60**, 15910 (1999).

[3] P.W. Fry, I. E. Itskevich, D. J. Mowbray, M. S. Skolnick, J. J. Finley, J. A. Barker, E.

P. O'Reilly, L. R. Wilson, I. A. Larkin, P. A. Maksym, M. Hopkinson, M. Al-Khafaji, J. P. R. David, A. G. Cullis, G. Hill, and J. C. Clark, Phys. Rev. Lett. **84**, 733 (2000).

[4] A. Patane, A. Levin, A. Polimeni, F. Schindler, P. C. Main, L. Eaves, and M. Henini, Appl. Phys. Lett. **77**, 2979 (2000).

[5] J. A. Barker and E. P. O'Reilly, Phys. Rev. B **61**, 13840 (2000).

[6] W. Sheng and J. P. Leburton, Phys. Rev. B **63**, 161301 (2001).

[7] W. Sheng and J. P. Leburton, Phys. Rev. Lett. **88**, 167401 (2002).

[8] M. Nirmal, B. O. Dabbousi, M. G. Bawendi, J. J. Macklin, J. K. Trautman, T. D. Harris, and L. E. Brus, Nature **383**, 802 (1996).

[9] N. H. Bonadeo, J. Erland, D. Gammon, D. Park, D. S. Katzer, and D. G. Steel, Science **282**, 1473 (1996).

[10] S. Takeoka, M. Fujii, and S. Hayashi, Phys. Rev. B **62**, 16820 (2000).

[11] C. G. Ahn, T. S. Jang, K. H. Kim, Y. K. Kwon, and B. Kang, Jpn. J. Appl. Phys. **42**, 2382 (2003).

[12] J. C. Cheang-Wong, A. Oliver, J. Roiz, J. M. Hernanaez, L. Rodriguez-Fernandez, J. G. Morales, and A. Crespo-Sosa, Nucl. Instr. And Meth. In Phys. Res. B **175-177**, 490 (2001).

[13] C. Itoh, T. Suzuki, and N. Itoh, Phys. Rev. B **41**, 3794 (1990).

[14] C. Itoh, K. Tanimura, N. Itoh, and M. Itoh, Phys. Rev. B **39**, 11183 (1989).

[15] G. Pacchioni, F. Frigoli, D. Ricci, and J. A. Weil, Phys. Rev. B **63**, 054102 (2000).

[16] C. Delerue, G. Allan, and M. Lannoo, Phys. Rev. B **48**, 11024 (1993).

[17] P. Mutti, G.. Ghislotti, S. Bertoni, G. F. Cerofolini, L. Meda, E. Grilli, and M. Guzzi, Appl. Phys. Lett. **66**, 851 (1995).

[18] Y. P. Varshni, Physica **34**, 149 (1967).

[19] Z. Ma, K. Pierz, Surf. Sci. **511**, 57 (2002).

[20] M. Koch, R. Hellmann, G. Bastian, J. Feldmann, E. O. Gobel, P. Dawson, Phys. Rev. B **51**, 13887 (1995).

[21] D. A. B. Miller, D. S. Chemla, T. C. Damen, A. C. Gossard, W. Wiegmann, T. H. Wood, and C. A. Burrus, Phys. Rev. Lett. **53**, 2173 (1984).

[22] I. Bar-Joseph, C. Kingshirn, D. A. B. Miller, D. S. Chemla, U. Koren, and B. I. Miller, Appl. Phys. Lett. **50**, 1010 (1987).

[23] K. Wakita, Y. Kawamura, Y. Yoshikuni, H. Asahi, and S. Uehara, IEEE J. Quantum Electron. **QE-22**, 1831 (1986).

[24] Y. Shi, J. H. Zhao, J. Sarathy, G. Olsen, and H. Lee, Electron. Lett. **33**, 248 (1997).

[25] S. H. Choi, and R. G. Elliman, Appl. Phys. Lett. **74**, 3987 (1999).